Nonlinear Optical Properties and Phototunable Absorption of a Substituted Dihydroazulene−Vinylheptafulvene Pair of Photochromes

Imene Bayach,*,|| Nadiah Almutlaq,|| Mohammed A. Alkhalifah, Misbah Asif, Khurshid Ayub,* and Nadeem S. Sheikh*

ACCESS | 📊 Metrics & More | 📰 Article Recommendations | 🆘 Supporting Information

ABSTRACT: Quantum calculations were used to study UV−vis absorption properties and nonlinear optical characteristics of a variety of substituted dihydroazulene (DHA)/vinylheptafulvene (VHF) photoswitches. The absorption properties are substantially based on the position and nature of the substituent. In general, electron-donating groups cause red shifts compared to the parent compound. Any electron-withdrawing group, on the other hand, would generate a blue shift. Furthermore, the steric effect at some positions is accountable for the loss of planarity and, as a response, a decrease in electronic conjugation within the molecule, which in most cases result in blue shifts in maximum absorption. The purpose of this research is to investigate the influence of substitution at the seven-membered ring of the DHA/VHF system on the absorption spectra and nonlinear optical characteristics of dihydroazulene photoswitches. UV−vis spectra and hyperpolarizability are determined since a prospective photoswitch should have a minimum overlap of absorption spectra from both isomers. Furthermore, the differential in hyperpolarizability between DHA and VHF is critical for practical applications.
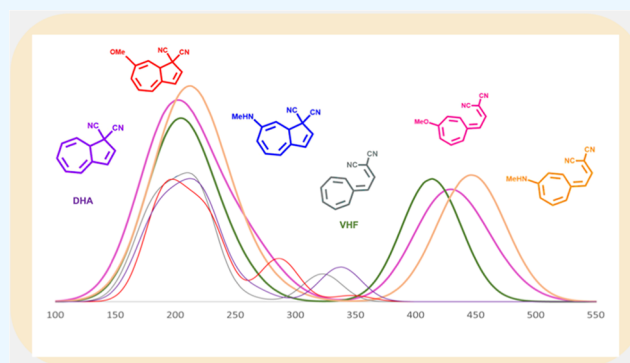
1. INTRODUCTION

Over the last three decades, scientists have paid more attention to molecular photoswitches[1] because they are used in a wide range of fields, such as nonlinear optics (NLO),[2−4] memory devices,[5,6] liquid crystals,[7−17] electromagnetic switches,[18−20] synthetic ion channels,[21,22] photopharmacology,[24] biological processes,[23] etc. In addition, a significant number of complicated devices, including encoder−decoder,[35] half adder,[25−33] and logic gates,[34] can be designed based on photoswitches. They have a distinctive feature associated with isomeric interconversion. In general, thermal stability, fatigue resistance, photochemical quantum yield, and nondestructive reading are all important factors that govern the efficiency of photoswitches. For applications in NLO and memory devices, photoswitches need only a minimal overlap between the absorption spectra of their respective isomeric states. This is necessary to prevent the formation of a photostationary state, which refers to an isomeric coexistence at equilibrium. Furthermore, for optimal performance, the polarizability variation within isomeric states should really be considered.

Among electronic-based photochromes, fulgides[36] and dithienylethenes[21] receive the greatest amount of attention because of their thermal stability. Another significant class is the dihydroazulene (DHA)/vinylheptafulvene (VHF) photochromic pair (Figure 1), which needs more study and has a

variety of practical applications. However, this class is less explored and needs further exploration. In comparison to its colored analogue VHF, DHA is a colorless molecule that has higher thermodynamic stability.[37−44] If these two isomers are exposed to light and/or heat, they will readily undergo interconversion. Vinylheptafulvene is composed of two conformers, s-trans and s-cis, which are in equilibrium, and interestingly, the s-cis conformer, which is created photochemically, is more stable than the s-trans conformer.[37−44] Significant obstacles that hinder the advancement of this class for industrial uses include thermal instability, which results in the conversion of VHF into DHA (T-type photoswitch),[45] and related synthetic difficulties.
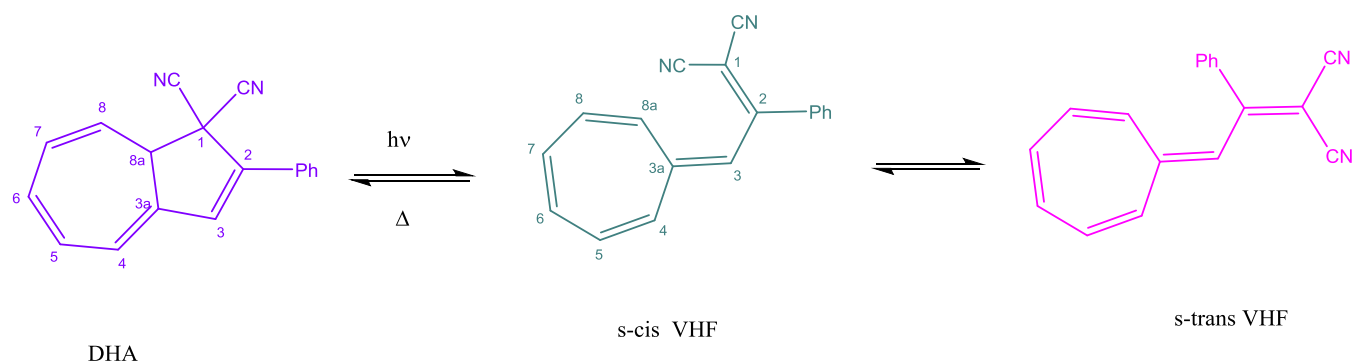
Efforts have been made to create multimode photoswitches by combining dithienylethenes and other photochromic materials with DHA−VHF photoswitches, and the properties of DHA/VHF have extensively been modulated.[46] Further-

Figure 1. Isomeric interconversion of DHA and VHF.

more, the correlation between the substitution effect and the physical properties of photoswitches has been extensively researched. Both the five- and seven-membered rings of DHA have been effectively modified by the introduction of appropriate functional atoms/groups.[47−49] However, considerable synthetic challenges prevent the seven-membered ring from being functionalized. Furthermore, as foreseen in the case of protonation of the amino group on phenylethynyl DHA X,[48] effective functionalization at the seven-membered ring has shown to bring a substantial advantage to DHA−VHF photoswitches. Under temperature circumstances, this resulted in the deactivation of VHF X to DHA X.

We have evaluated the electocyclization activation barriers and the features of DHA−VHF photoswitches computationally in order to get a deeper understanding of how substituents affect the reactivity pattern.[50] It was observed that the arrangement and the type of the substituents on the seven-membered rings had a significant influence on the electronic properties of DHA−VHF photoswitches by conducting thermal return reactions for various substituted VHFs to DHFs. Furthermore, a significant change (up to 7 kcal mol^{-1}) was reported for electrocyclization by changing the arrangement and the type of substituents. As an example, the thermal cyclization of 5-OH VHF to DHA has an energy barrier of 23.7 kcal mol^{-1}, whereas the energy barrier for 4-OH VHF is 30.5 kcal mol^{-1}. The electron-withdrawing group, on the other hand, causes the opposite tendency. The activation barrier required to cause the cyclization of 5-CHO VHF is 29.5 kcal mol^{-1}, which is higher than the activation energy for 5-OH VHF, which is 23.7 kcal mol^{-1}. A similar trend is provided by the occurrence of other groups at position 7 of VHF.[48] We have recently reported the effect of several substituents on the seven-membered ring of the DHA−VHF system on different positions in the photophysical properties of this system through structural modification.[51] We have reported that any electron-donating group would cause the maximum red shift of the VHF absorption spectra, whereas any electron-withdrawing group would cause the maximum blue shift of the VHF absorption spectra (Table S1).

In our ongoing research on establishing a structure−property relationship of substituted DHA−VHF for UV−vis spectra and NLO switches,[52] we report here a thorough study to investigate the influence of other substituents on DHA's seven-membered ring and their effects. The object of this extensive theoretical study is to further investigate the photophysical properties of DHA−VHF by structural modification and to establish a general and clear structure/activity relationship. In addition, the current study includes the

computation of hyperpolarizabilities, as the difference in hyperpolarizability between the two isomers should be considered for their practical application in nonlinear optical devices.

2. COMPUTATIONAL METHODS

Gaussian09 was used to carry out the calculation.[53] All structural geometries were optimized at the PBE1PBE/6-311+G(d) level of theory without any symmetry restrictions. The PBE1PBE method accurately predicts organic dye structural characteristics, particularly DHA−VHF, at a low cost.[50] In our previous report, we also showed that the geometries and energies of DHA/VHF at the PBE0 method agree well with the results of the experiment.[50] Additionally, frequency calculations were done at PBE1PBE/6-311+G(d) to establish the structures as true minima (no imaginary frequency). The UV−vis spectra are calculated using TD-DFT on PBE1PBE/6-311+G(d)-optimized structures at the CAM-B3LYP/6-311+G(d) level of theory. The absorption maxima that have been reported are those that occur at maximum wavelengths with oscillator strengths higher than 0.2. The CAM-B3LYP/6-311+G(d) level of theory is also used to determine the hyperpolarizability values, which give good agreement between computational cost and accuracy.

In order to determine the first hyperpolarizability (β), we used the following formula, as reported in the literature[54]

$$\beta_o = [(\beta_{xxx} + \beta_{xyy} + \beta_{xzz})^2 + (\beta_{yyy} + \beta_{yzz} + \beta_{yxx})^2 + (\beta_{zzz} + \beta_{zxx} + \beta_{zyy})^2]^{1/2}$$

It should be noted that the values of hyperpolarizability are dependent on the frequency of the electric field. Our calculation included both static hyperpolarizability and second-order nonlinear optical properties, first hyperpolarizability (β) according to the given formula.[54]

3. RESULTS AND DISCUSSION

Organic photochromes have many applications, but their thermal stability determines their practical application. For ideal photochromes, there should be no spectral overlap between the two isomeric species in the UV−vis region, and the switching process should be photocontrolled only. A spectral overlap causes incomplete interconversion of both isomers, resulting in the creation of a photostationary state. In the photostationary state, the relative concentration of both components is determined by the irradiation wavelength, thermal return rate, and irradiation time.[55] The objective of

Table 1. λ_{high} and λ_{max} for DHAs and VHFs (Electron-Donating Groups—*⟨C2−C3−C3a−C8 of DHAs⟩)

no.	substituents	DHA (λ_{high}) (λ_{max})	$f > 0$	dihedral angle*	VHF (λ_{high}) (λ_{max})	$f > 0$
1	8a-PH$_2$	361	0.08	−22.62	412	0.39
		226	0.24			
2	8-PH$_2$	318	0.11	−50.69	440	0.05
		226	0.27		429	0.46
3	7-PH$_2$	315	0.16	−41.48	427	0.20
		222	0.40		408	0.40
4	6-PH$_2$	318	0.20	−40.11	424	0.03
		219	0.47		414	0.64
5	5-PH$_2$	314	0.11	−40.65	423	0.14
		222	0.73		416	0.49
6	4-PH$_2$	313	0.12	−43.77	417	0.10
		220	0.60		404	0.42
7	8a-OMe	328	0.15	−12.18	434	0.47
		213	0.36			
8	8-OMe	327	0.13	−47.62	478	0.01
		218	0.21		427	0.49
9	7-OMe	329	0.08	−37.32	456	0.04
		221	0.30		439	0.55
10	6-OMe	343	0.20	−40.37	472	0.06
		224	0.38		433	0.56
11	5-OMe	343	0.10	−43.73	434	0.13
		222	0.41		409	0.49
12	4-OMe	345	0.15	−39.43	428	0.52
		235	0.43			
13	8a-NHMe	338	0.13	−11.41	474	0.37
		217	0.23		272	0.40
14	8-NHMe	359	0.13	−49.66	503	0.03
					443	0.42
15	7-NHMe	347	0.02	−39.47	452	0.60
		290	0.22			
16	6-NHMe	348	0.26	−37.91	484	0.12
					444	0.52
17	5-NHMe	347	0.06	−42.30	500	0.01
		234	0.75		427	0.66
18	4-NHMe	354	0.16	−42.72	465	0.51
		248	0.22			
19	8a-NMe$_2$	337	0.00	−32.22	481	0.31
		218	0.51		281	0.40
20	8-NMe$_2$	376	0.08	−45.56	467	0.11
		243	0.34		432	0.34
21	7-NMe$_2$	345	0.01	−39.93	460	0.59
		294	0.23			
22	6-NMe$_2$	344	0.31	−39.62	465	0.37
23	5-NMe$_2$	362	0.06	−45.18	468	0.05
		239	0.79		430	0.63
24	4-NMe$_2$	371	0.13	−45.30	455	0.42
		256	0.14			
25	8a-CH$_2$OH	339	0.12	−26.38	424	0.46
		226	0.40			
26	8-CH$_2$OH	317	0.12	−49.89	430	0.14
		223	0.27		414	0.38
27	7-CH$_2$OH	323	0.13	−35.93	429	0.15
		221	0.45		413	0.41
28	6-CH$_2$OH	320	0.18	−40.51	430	0.06
		221	0.38		417	0.57
29	5-CH$_2$OH	320	0.12	−41.10	428	0.01
		220	0.62		416	0.61
30	4-CH$_2$OH	318	0.13	−42.75	421	0.21
		221	0.43		408	0.36
31	8a-CH$_2$NH$_2$	362	0.09	−14.35	422	0.45
		228	0.24			

Table 1. continued

no.	substituents	DHA (λ_{high}) (λ_{max})	$f > 0$	dihedral angle*	VHF (λ_{high}) (λ_{max})	$f > 0$
32	8-CH$_2$NH$_2$	318	0.12	−46.63	432	0.23
		221	0.29		421	0.32
33	7-CH$_2$NH$_2$	319	0.13	−40.06	426	0.27
		219	0.39		419	0.34
34	6-CH$_2$NH$_2$	322	0.18	−39.54	424	0.01
		221	0.40		418	0.64
35	5-CH$_2$NH$_2$	320	0.12	−39.31	426	0.07
		221	0.53		414	0.55
36	4-CH$_2$NH$_2$	323	0.13	−44.36	451	0.02
		223	0.42		421	0.53
37	8a-CH$_2$F	346	0.12	−17.45	419	0.44
		220	0.30			
38	8-CH$_2$F	318	0.12	−48.44	428	0.09
		219	0.37		419	0.45
39	7-CH$_2$F	318	0.14	−41.02	428	0.11
		219	0.48		407	0.48
40	6-CH$_2$F	318	0.18	−39.62	427	0.01
		218	0.51		412	0.61
41	5-CH$_2$F	315	0.11	−40.29	427	0.01
		219	0.69		412	0.60
42	4-CH$_2$F	319	0.13	−44.07	447	0.01
		218	0.51		412	0.53
43	8a-CH$_2$Cl	352	0.11	−12.41	421	0.42
		221	0.21			
44	8-CH$_2$Cl	325	0.10	−48.02	426	0.14
		222	0.42		419	0.42
45	7-CH$_2$Cl	318	0.14	−40.85	432	0.13
		221	0.49		409	0.49
46	6-CH$_2$Cl	322	0.21	−39.77	430	0.03
		220	0.50		414	0.64
47	5-CH$_2$Cl	317	0.11	−40.63	424	0.02
		222	0.81		413	0.60
48	4-CH$_2$Cl	322	0.13	−44.16	450	0.01
		224	0.52		413	0.53
49	8a-CH$_2$Br	354	0.10	−11.32	427	0.38
		234	0.16			
50	8-CH$_2$Br	333	0.09	−47.84	428	0.08
		227	0.42		423	0.48
51	7-CH$_2$Br	318	0.14	−40.90	437	0.15
		224	0.46		411	0.48
52	6-CH$_2$Br	326	0.25	−39.77	434	0.06
		219	0.47		416	0.64
53	5-CH$_2$Br	319	0.10	−40.70	424	0.02
		230	0.55		413	0.60
54	4-CH$_2$Br	324	0.14	−44.24	457	0.02
		222	0.28		416	0.52

this study is to investigate the substituents that result in a spectral nonoverlap when added to the DHA−VHF system.

Considering the fact that DHA and VHF both absorb in the UV and visible spectral regions, a spectral nonoverlap can be achieved more effectively if the UV−vis spectra of DHA and VHF are, respectively, blue- and red-shifted. The UV−vis spectra of DHA and VHF have been extensively studied both experimentally and theoretically. Jacquemin and co-workers used a benchmark approach to study the UV−vis spectra of DHA and VHF using the CAM-B3LYP, B97XD, and PBE0 methods with different basis sets.[56] The absorption maximum shift from phenyl DHA (1) (354 nm) to VHF (2) (459 nm) was measured experimentally to be 105 nm, while calculated

differences at CAM-B3LYP, PBE0, and B97XD were 87, 87, and 90 nm, respectively. Figure 1 shows the simplified unsubstituted DHA and VHF. To support our decision to use the same approach in this study, they have calculated the UV−vis spectra of the DHA−VHF pair and found that the CAM-B3LYP method provided the most accurate simulation.

3.1. Substitution Effect on the UV−Vis Spectra of VHF. Different functional groups are tested to see how they influence the UV−vis spectra of the DHA−VHF pair. The studied functional groups are described in detail in Tables 1 and 2 and S2. These groups are highly diversified, encompassing electron donor and acceptor groups, both mesomerically and inductively. It is difficult to separate these

Table 2. λ_{high} and λ_{max} for DHAs and VHFs (Electron-Withdrawing Groups—*⟨C2−C3−C3a−C8 of DHAs)

no.	substituents	DHA (λ_{high}) (λ_{max})	$f > 0$	dihedral angle*	VHF (λ_{high}) (λ_{max})	$f > 0$
1	8a-C(O)Me	327	0.12	−33.41	419	0.06
		221	0.42		380	0.33
2	8-C(O)Me	341	0.10	−48.07	447	0.10
		230	0.58		422	0.39
3	7-C(O)Me	324	0.10	−40.82	467	0.10
		233	0.27		409	0.50
4	6-C(O)Me	339	0.19	−39.91	472	0.08
		218	0.42		412	0.60
5	5-C(O)Me	341	0.05	−41.78	455	0.24
		235	0.80		412	0.37
6	4-C(O)Me	334	0.09	−45.53	416	0.07
		237	0.45		385	0.38
7	8a-CO$_2$Me	320	0.14	−32.97	417	0.11
		220	0.39		378	0.29
8	8-CO$_2$Me	331	0.11	−47.83	447	0.18
		225	0.62		422	0.34
9	7-CO$_2$Me	324	0.11	−41.08	465	0.09
		226	0.52		407	0.52
10	6-CO$_2$Me	337	0.22	−40.14	460	0.09
		216	0.47		409	0.59
11	5-CO$_2$Me	331	0.09	−39.47	457	0.19
		227	0.87		414	0.44
12	4-CO$_2$Me	326	0.13	−44.99	421	0.04
		229	0.55		394	0.45
13	8a-C(O)NH$_2$	321	0.13	−35.09	417	0.18
		220	0.27		380	0.22
14	8-C(O)NH$_2$	325	0.11	−46.64	446	0.19
		222	0.49		432	0.34
15	7-C(O)NH$_2$	326	0.13	−37.81	464	0.04
		224	0.54		415	0.58
16	6-C(O)NH$_2$	328	0.22	−40.61	457	0.04
		217	0.38		409	0.62
17	5-C(O)NH$_2$	330	0.10	−37.61	444	0.15
		226	0.77		413	0.47
18	4-C(O)NH$_2$	324	0.13	−44.83	440	0.02
		222	0.61		411	0.52
19	8a-C(O)Cl	320	0.13	−30.96	419	0.04
		221	0.48		377	0.35
20	8-C(O)Cl	346	0.11	−48.52	454	0.19
		232	0.59		414	0.30
21	7-C(O)Cl	324	0.09	−41.96	486	0.08
		232	0.43		400	0.52
22	6-C(O)Cl	344	0.25	−40.75	469	0.12
		215	0.34		400	0.56
23	5-C(O)Cl	336	0.07	−40.10	478	0.19
		235	0.88		410	0.43
24	4-C(O)Cl	333	0.13	−45.87	421	0.08
		238	0.44		380	0.39

groups according to their nature; therefore, the discussion in the following part is divided according to their electronic nature.

3.1.1. Mesomerically Electron-Donating Groups. The calculated UV−vis absorption spectra have a typical form with two peaks; we are interested in the near visible one, which is associated with the third excited state and is primarily defined by the HOMO (51)−LUMO (52) electronic transition (Table S2). The investigation of other excited states clearly shows that another transition, defined by maximum high wavelengths (λ_{high}), is possible at positions 5, 6, and 8. In

our most recent work, we evaluated some electron-donating groups including NH$_2$, OH, SiH$_3$, and SH on the seven-membered ring of VHF.[51] In the current work, we are evaluating the introduction of different substituents in the seven-membered ring of VHF, as shown in the following tables.

The introduction of the PH$_2$ substituent in the seven-membered ring of VHF did not prove meaningful because the absorption of maximum wavelength for most derivatives was quite comparable to the parent VHF (Figure 2B). This is due to the nonparticipation of the lone pair of electrons belonging
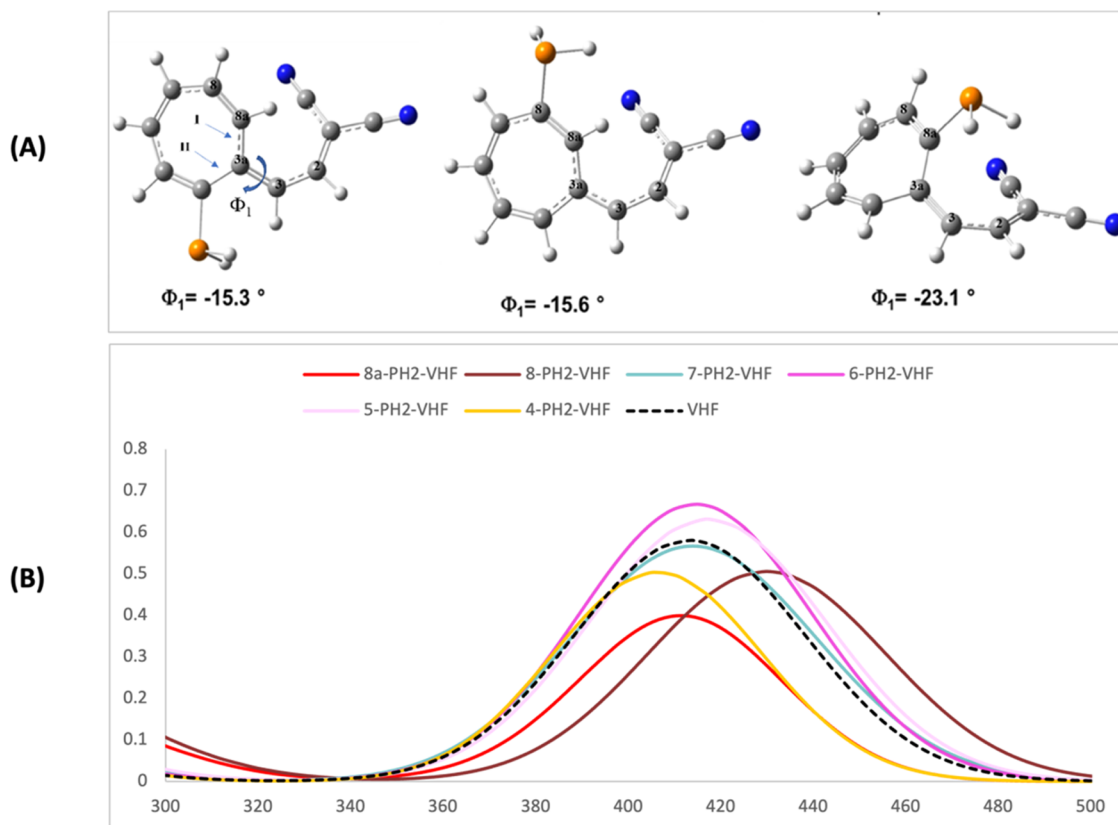
Figure 2. (A) Optimized structures for 4-, 8-, and 8a- PH_2 VHF photoswitches indicating Φ_1 and (B) their calculated UV−vis spectra.
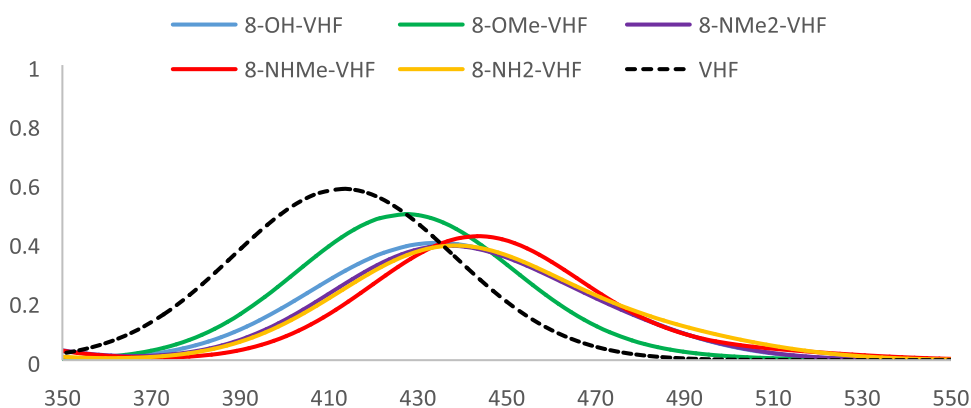
Figure 3. Calculated UV−vis spectra for selected 8-substituted VHFs.

to phosphorus in the conjugation for all positions. For 8a-, 7-, and 4-PH_2VHFs, the absorption spectra are even blue-shifted (although by 1, 5, and 9 nm, respectively), which could be attributed to the loss of planarity and interruption of conjugation from both pathways I and II and from the donor group (PH_2) (Figure 2A). The blue shift is more pronounced for λ_{max} at these positions (Figure 2B).

When PH_2 is compared to electron-donating substituents (NH_2, OH, SiH_3, SH) that have been studied in our most recent work[51] (Figure S1), it can be clearly seen that stronger electron-donating substituents have the greatest effect. Indeed, NH_2 has the highest red shift, especially at position 8a, followed by OH and SH with similar behaviors, whereas the PH_2 effect is the weakest. In general, mesomeric electron-donating groups on VHF generated a red shift in the absorption spectra, with the amount of the effect depending

on the position of the functional group besides the nature of the electron-donating group (Table 1).

Next, the effect of methylation of NH_2 and OH on the UV−vis spectra is analyzed (Table 1). Comparison of the results reveals that, for the NH_2 substituent, methylation generally causes a red shift in the absorption spectra (Figure S2), except at position 8a, where the steric effect has induced a hypsochromic shift with the increase of substitution (i.e., from −NH2 → −NHMe → −NMe$_2$) (Figure S3-A). In fact, the absorption of maximum wavelength in 8a-NHMe VHF and 8a-NMe$_2$ VHF is 272 and 281 nm, respectively, compared to 471 nm for 8a-NH$_2$ VHF. Similarly, at positions 4 and 8, the second methylation induced a blue shift, while a red shift is observed for the first methylation, which may be due to steric crowding for second methylation, which hinders the proper overlap between the substituent and the VHF ring. The
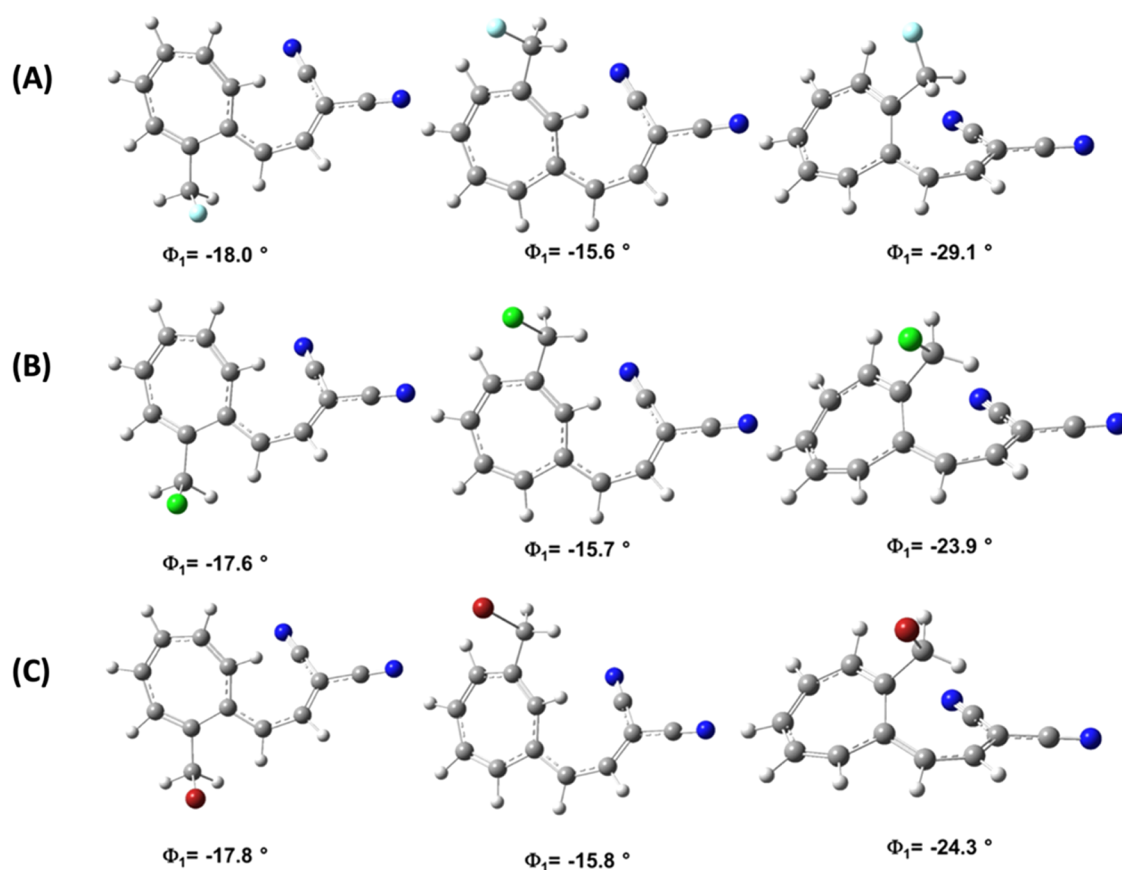
Figure 4. Geometric properties for (A) F, (B) Cl, and (C) Br halomethyl-substituted VHFs including Φ.

absorption of maximum wavelength at all other positions increases with methylation. However, the gain of donating power due to methylation induces a red shift for λ_{high} for all positions including 8a and 4 (Table 1).

Methylation of the OH group (to OMe) causes red shifts in the UV−vis spectra for positions 5, 6, and 7, while blue shifts are observed for O-methylation at positions 4, 8, and 8a (Figure S4). As described previously, the blue shift observed for methylation at 4, 8, and 8a positions could be ascribed to the steric effect, the decrease in participation of the lone pairs of electrons with the seven-membered ring of VHF, and the loss of planarity (Figure S3-B). Moreover, at position 8a, the lone pair of the substituent shows through space interactions with nitrile carbon. This interaction is slightly stronger for methoxy-substituted VHF (2.7 Å) compared to OH-substituted VHF (2.9 Å). An interesting situation is observed for methylation of NH_2 and OH at position 8, where a red shift is observed for monomethylation of NH_2, whereas a blue shift is observed for dimethylation of NH_2, and a nonsignificant effect for methylation of OH (Figure 3). From these results, it can be inferred that methylation causes a red shift in the UV−vis spectrum unless there is some reduction in the delocalization of electrons caused by methylation. Also, it is important to clarify that methylation at all positions induced a red shift when the UV−vis spectra are compared to the parent VHF instead of hydroxylated VHF.

Next, the effect of deprotonation on the UV−vis spectra is studied (Table S3). As expected, the deprotonation led to a remarkable red shift in the UV−vis spectra for ($S^{(−)}$, $O^−$, NH_3^+, and PH_3^+) substituted VHFs, particularly for mercapto-substituted VHFs. The maximum red shift is observed for 4-

$S^{(−)}$ VHF, where the absorption of maximum wavelength is calculated at 502 nm. The wavelength is red-shifted by 73 nm when compared with 4-SH VHF. However, the lowest red shift is found for 8a with λ_{max} of 324 nm. When we take into account λ_{high}, 8a has the greatest effect (519 nm). For $S^{(−)}$ at other positions, the transitions are observed between 445−491 nm, which are, on average, 45 nm red-shifted when compared with their corresponding SH-substituted VHFs (Figure S5).

A similar but less pronounced effect is seen when the OH group is deprotonated to $O^{(−)}$. Among $O^{(−)}$-substituted VHFs, the maximum red-shifted spectrum is calculated for 8a-$O^{(−)}$ VHF (478 nm). The UV−vis spectrum of this compound is red-shifted by 17 nm when compared with 8a-OH VHF. The next highest wavelength is seen for 4-$O^{(−)}$ (473 nm), quite analogous to $S^{(−)}$ VHFs. For 5, 6, 7, and 8-$O^{(−)}$ VHFs, the absorption maxima are calculated between 382−458 nm, all red-shifted when compared with their protonated analogues. Again, the electron pair of the thiolate anion is not involved in conjugation (Figure S6).

3.1.2. Substituted Methyl Functional Groups. Our previous study[51] has shown that the methyl substituent has little effect on the UV−vis spectrum (Table 1). Also, a comparison of methyl and silyl groups revealed that substitution at positions 6 and 8 have the maximum red shift in the absorption spectrum.[51] In the present study, we have introduced halomethyl substituents and showed that the effect of halogen atoms is quite subtle. In general, the UV−vis spectra of halomethyl-substituted VHFs are very comparable to those of methyl VHFs. The effect of a halogen on methyl depends on the nature of the halogen. For all halomethyl groups, blue shifts were observed at all positions except 8 and 4 when compared

to methylated analogues (Table 1). When we compared the effect according to λ_{high}, we found that strongly electron-withdrawing fluorine (Figure S7) induces a blue shift at all positions except 7 (428 nm) and 4 (447 nm). In the case of weakly withdrawing bromine (Figure S8), a slight red shift is observed at all positions, except at 8 (428 nm) and 5 (424 nm). For intermediate chlorine, a slight red shift is observed at 4 (450 nm), 6 (430 nm), and 7 (432 nm) (Figure S9). Otherwise, when we compared the effect according to λ_{max}, we found the same cases. For example, the absorption of maximum wavelength is shifted to 419 nm in 8a-CH$_2$F VHF compared to 423 nm for methyl VHF at the same position. A decrease in blue shift is observed for 8a-CH$_2$Cl VHFs with an average of 13 nm compared with methyl VHFs at the same position. For CH$_2$Br at position 8a, the calculated wavelength is 427 nm, which is about 4 nm red-shifted compared to 8a-CH$_3$ VHF. A similar trend is observed for 7-CH$_2$X VHF, where the absorption values are 407, 409, and 411 nm for CH$_2$F, CH$_2$Cl, and CH$_2$Br, respectively, compared to 418 (426) nm for CH$_3$ VHF. For 6-CH$_2$X VHF, the absorption maxima are blue-shifted when compared with Me VHF at position 6, although the blue shift decreases with an increase in the atomic number of halogens. To summarize, the blue shift caused by halomethyl on absorption wavelengths increases with the electronegativity of halogens. Finally, structural analysis of halomethyl substituents revealed similar effects on positions 8a and 4, where the conjugation is disconnected from one of the two possible pathways (Figure 4).

Similarly, investigation of UV−vis spectra for CH$_2$NH$_2$- and CH$_2$OH-substituted VHFs revealed trends very comparable to those of methyl VHFs. Regarding CH$_2$NH$_2$ VHFs, when we compared the effect with methylated VHF according to λ_{max}, the absorption maxima are red-shifted at all positions, except positions 8a and 5 are slightly blue-shifted, and a nonsignificant effect is observed at position 6. However, based on λ_{high}, only the CH$_2$NH$_2$ group at position 4 (451 nm) induced a red shift in the absorption spectrum, while at position 7 (426 nm), the wavelength was unaffected, and at all other positions induced a blue effect (Figure S10). Conversely, according to λ_{max}, the introduction of CH$_2$OH at positions 4, 7, and 8 induces a blue shift of 2, 5, and 2 nm, respectively (Figure S11). Also, an opposite effect was observed for the CH$_2$OH group at position 8a, for which maximum absorption is now slightly red-shifted (1 nm) compared to the methylated analogue (8a-Me VHF). The maximum wavelength at position 6 (6-CH$_2$OH VHF) is unchanged compared to its methylated analogue (6-Me VHF).

By comparing the global shapes of UV−vis spectra for CH$_2$NH$_2$ and CH$_2$OH VHFs, the effect compared to methylated VHFs is minor generally with a slightly more pronounced red shift for amino-substituted VHFs compared to hydroxyl-substituted VHFs, which is comparable to that observed for NH$_2$- and OH-substituted VHFs. Conversely, 5 and 8a positions revealed an opposite, which may be attributed to the same reasons as for halomethyl substituents (Figure S12).

3.1.3. Electron-Withdrawing Substituents.

All of the electron-withdrawing groups (EWGs) that have been studied act very similarly, and some tendencies may be simply identified (Table 2). As previously stated, there are two transitions in the parent VHF scaffold (413 and 438 nm). In most cases, the presence of an electron-withdrawing group substituent results in a red shift of the peak at 438 nm and a blue shift of the peak at 413 nm. However, there is an exception for positions 4 and 8a (Table 2, see below), where blue-shifting is recognized for both peaks. This finding is in conformance with our previous inferences regarding these two specific positions. In our previous study,[51] we tested some relatively strong electron-withdrawing groups such as NO$_2$, CN, C(O)H, and COOH.[51] We also analyzed C(O)Me, COOMe, C(O)NH$_2$, and C(O)Cl to generalize these findings to larger EWGs (Table 2). In all positions, the introduction of any EWG causes a blue shift in the absorption spectra, except at position 8, where red shifts are seen. However, we observed that the substituent with the maximum hypsochromic effect at position 4 is COCl (380 nm), whereas CONH$_2$ has the lowest effect. The effect for all withdrawing groups at positions 5 and 6 is similar. Moreover, here again, we confirmed the effect of methylation, which leads to a red shift of λ_{max} at all positions except 8a-COMe due to a steric effect, as previously discussed. This is also applicable for comparing amide-, ketone-, and haloformyl-substituted VHFs, which are classified from the most red-shifting to the most blue-shifting groups, respectively (according to their respective donating powers (Table 2)). In addition, the structural analysis indicated that the insertion of any EWG at positions 8a and 4 resulted in discontinuous electronic conjugations at both pathways I and II (Figures S13 and S14).

3.2. Substitution Effect on the UV−Vis Spectra of DHA.

The position of substitution is what determines whether or not electron-donating or neutral moieties will have an influence on the UV−vis spectra (Table 1). We previously studied the effect of some electron-donating substituent (NH$_2$, OH, SiH$_3$, SH) DHAs.[51] In the current study, a similar behavior is found for PH$_2$-substituted DHAs, where a higher red shift is observed for 8a- and 8-PH$_2$ DHA (226 nm); however, this effect is nonsignificant for all other positions. When we compared the substitution effect on λ_{high} of PH$_2$ to other substituents that have been studied in our previous work (NH$_2$, OH, SiH$_3$, SH), blue shifts were observed for all other positions except for 8a (361 nm). Quite a resemblance in the behavior of PH$_2$ DHA with SiH$_3$ and Me DHAs reflects that the PH$_2$ moiety is not communicating with the DHA skeleton (Figure S15). Otherwise, the effect of PH$_2$ would be similar to NH$_2$ and other mesomeric donating substituents (vide infra).

Quite a significant red shift was observed when negative charge-bearing species were introduced to the DHA skeleton. The maximum effect was found for λ_{high} at position 7 in which the maximum wavelengths are 285 and 286 nm red-shifted for O$^-$- and S$^-$-substituted DHA, respectively, compared to the protonated congeners OH and SH (when this shift is compared to the parent DHA, the values are +296 and +297 nm for 4-O$^-$- and 4-S$^-$-substituted DHA, respectively). Interestingly, only at that position, we detected the two peaks of O$^-$-substituted DHA; at all other positions, only one peak was observed with considerable red-shifting; however, for S$^-$-substituted DHA, two peaks were detected at all positions, also significantly red-shifted. Conversely, the introduction of positive charge-bearing species NH$_3^+$ on the DHA skeleton generally induced a blue shift. However, for position 8a-NH$_3^+$ DHA, a slight red shift (λ_{max} = 223 nm) was observed, which can be explained by the gain of planarity and extension of conjugation at that structure (Figure S16). Moreover, the introduction of PH$_3^+$ induces less remarkable but still appreciable red shifts of absorption wavelengths at all positions. The larger wavelength is found for 8-PH$_3^+$ DHA

Table 3. Hyperpolarizability Values for DHAs and VHFs (Electron-Donating Groups)

no.	substituents	DHA	VHF	no.	substituents	DHA	VHF
1	8a-PH$_2$	1.40	11.09	31	8a-CH$_2$NH$_2$	1.60	9.48
2	8-PH$_2$	1.37	10.71	32	8-CH$_2$NH$_2$	1.16	8.54
3	7-PH$_2$	0.70	11.37	33	7-CH$_2$NH$_2$	1.38	13.80
4	6-PH$_2$	2.17	11.96	34	6-CH$_2$NH$_2$	3.36	13.53
5	5-PH$_2$	2.08	12.40	35	5-CH$_2$NH$_2$	1.18	13.81
6	4-PH$_2$	1.83	12.25	36	4-CH$_2$NH$_2$	0.73	11.10
7	8a-OMe	0.99	10.05	37	8a-CH$_2$F	1.54	9.26
8	8-OMe	2.65	4.44	38	8-CH$_2$F	1.27	11.07
9	7-OMe	2.74	13.40	39	7-CH$_2$F	1.39	13.61
10	6-OMe	9.09	16.30	40	6-CH$_2$F	1.32	14.41
11	5-OMe	4.26	15.59	41	5-CH$_2$F	0.84	14.80
12	4-OMe	2.49	15.53	42	4-CH$_2$F	1.35	11.94
13	8a-NHMe	1.42	11.04	43	8a-CH$_2$Cl	1.31	12.53
14	8-NHMe	4.91	13.01	44	8-CH$_2$Cl	1.20	10.65
15	7-NHMe	3.32	18.19	45	7-CH$_2$Cl	0.53	14.56
16	6-NHMe	14.10	15.02	46	6-CH$_2$Cl	0.41	12.64
17	5-NHMe	5.45	13.20	47	5-CH$_2$Cl	0.55	16.01
18	4-NHMe	4.26	7.74	48	4-CH$_2$Cl	0.98	11.67
19	8a-NMe$_2$	1.53	4.28	49	8a-CH$_2$Br	1.12	12.01
20	8-NMe$_2$	4.17	6.08	50	8-CH$_2$Br	1.09	9.52
21	7-NMe$_2$	4.08	16.47	51	7-CH$_2$Br	1.20	13.56
22	6-NMe$_2$	14.75	19.48	52	6-CH$_2$Br	2.99	12.00
23	5-NMe$_2$	6.99	18.26	53	5-CH$_2$Br	2.46	15.76
24	4-NMe$_2$	3.74	19.48	54	4-CH$_2$Br	2.64	11.86
25	8a-CH$_2$OH	1.68	7.40	28	6-CH$_2$OH	1.71	15.91
26	8-CH$_2$OH	1.54	10.56	29	5-CH$_2$OH	2.18	13.81
27	7-CH$_2$OH	2.24	12.85	30	4-CH$_2$OH	1.63	11.64

(352 nm), which is 34 nm red-shifted compared to its PH$_2$ congener.

Methylation of OH and NH$_2$ groups has led to either blue or red shifts or almost unchanged absorption spectra, depending on positions and number of methylations. Monomethylation of OH and NH$_2$ causes a red shift in the UV−vis spectrum in comparison to their OH and NH$_2$ congeners when these substituents occur at all positions (4, 5, 6, and 8a), except 8-OMe and 7-OMe DHA that cause a blue shift. For example, the absorption of the maximum wavelength for 8a-OMe DHA is 328 nm compared to 319 for 8a-OH DHA. The red shift is attributed to the increase in planarity. The *⟨C2−C3−C3a−C8 angle in 8a-OMe DHA is −12.18° compared to −22.87 for 8a-OH DHA. Also, for monomethylated NH$_2$, all positions cause a red shift in the UV−vis spectrum compared to their NH$_2$ congeners, except at position 8. The dimethylation of NH$_2$ increases the red shift at positions 4, 5, 6, and 8 compared to monomethylated congeners. A similar condition is found with 8a-NHMe and 8a-NMe$_2$ DHAs, where maximum wavelength absorption occurs at 338 and 337 nm for 8a-NHMe and 8a-NMe$_2$ DHAs, respectively. For 4-NHMe and 4-NMe$_2$ DHAs, the absorption maxima are 354 and 371 nm, respectively, compared to 352 for 4-NH$_2$ DHA. An interesting situation is observed for methylation of the substituent at position 8, where a red shift is observed for methylation of NH$_2$ (10 nm), whereas a blue shift (7 nm) is observed for O-methylation. The effect of N-methylation is negligible at 6 and 7, while O-methylation induces a 5 nm bathochromic shift at 6 and 5 nm hypsochromic shifts at 7.

CH$_2$NH$_2$- and CH$_2$OH-substituted DHAs showed different effects depending on the position. The most significant effect is a bathochromic shift of λ_{high} observed at position 8a (+39 and

+16 nm for 8a-CH$_2$NH$_2$ and 8a-CH$_2$OH DHAs, respectively). This shift gets higher for the stronger electron-donating groups. The introduction of CH$_2$NH$_2$ and CH$_2$OH groups at all positions led to red-shifted absorption spectra. However, λ_{high} values are decreased when CH$_2$NH$_2$ and CH$_2$OH are introduced at positions 5, 6, and 8. Finally, the effects induced by CH$_2$NH$_2$ and CH$_2$OH at 4 and 7 positions are different; high wavelengths for 4-CH$_2$NH$_2$- and 7-CH$_2$OH-substituted DHAs are unchanged (323 nm), while 7-CH$_2$NH$_2$ and 4-CH$_2$OH are 4 and 5 nm blue-shifted, respectively (compared to the parent DHA).

Regarding CH$_2$X-substituted DHAs, the effect of the additional X group generally causes a slight red shift of λ_{max}, while the effect on λ_{high} is dependent on the nature of the halogen. For the strong electron-withdrawing fluoro group, a blue shift is observed in the UV−vis spectrum except for 8a-CH$_2$F DHA, which shows a red shift of +23 nm (quite similar to 8a-Me DHA (+13 nm)) due to the loss of planarization of the scaffold. The red shift in the UV−vis spectrum for 8a-CH$_2$X gets higher for larger halogens (+29 and +31 nm for Cl and Br, respectively). For 8a-CH$_2$Cl DHA, the absorption of the high wavelength appears at 352 nm, where it is further red-shifted to 354 nm for 8a CH$_2$Br DHA. The increase in red shift with an increase in the atomic number of the halogen is attributed to two factors; a gain in planarity and a decrease in electronegativity of the halogen. The red shift is more pronounced for CH$_2$NH$_2$, where the electron-donating power is higher than the CH$_2$-halogen group. The absorption in 8a-CH$_2$NH$_2$ DHA appears at 362 nm. For all CH$_2$X substituents (except for 8-CH$_2$Cl, 8-CH$_2$Br, 6-CH$_2$Br, and 4-CH$_2$Br), blue shifts are observed when these groups are present at positions 4−8, which is very much consistent with

Table 4. Hyperpolarizability Values for DHAs and VHFs (Electron-Withdrawing Groups)

no.	substituents	DHA	VHF	No.	substituents	DHA	VHF
1	8a-C(O)Me	1.48	12.28	13	8a-C(O)NH2	1.57	12.65
2	8-C(O)Me	2.10	11.48	14	8-C(O)NH2	1.32	9.13
3	7-C(O)Me	0.76	11.76	15	7-C(O)NH2	1.81	13.73
4	6-C(O)Me	4.99	8.02	16	6-C(O)NH2	1.75	12.86
5	5-C(O)Me	2.19	6.88	17	5-C(O)NH2	1.11	11.45
6	4-C(O)Me	2.26	14.15	18	4-C(O)NH2	0.69	14.37
7	8a-CO2Me	1.12	13.11	19	8a-C(O)Cl	0.99	11.49
8	8-CO2Me	0.80	12.47	20	8-C(O)Cl	2.63	13.50
9	7-CO2Me	0.63	12.49	21	7-C(O)Cl	0.96	10.73
10	6-CO2Me	2.92	10.87	22	6-C(O)Cl	7.28	5.74
11	5-CO2Me	1.31	10.58	23	5-C(O)Cl	3.59	6.64
12	4-CO2Me	0.97	16.15	24	4-C(O)Cl	2.52	13.27

the behavior of the corresponding methyl DHAs. Red shifts of 2, 10, 3, and 1 nm are observed for 8-CH_2Cl, 8-CH_2Br, 6-CH_2Br, and 4-CH_2Br DHAs, respectively.

In general, UV−vis spectra have a negligible effect on the seven-membered ring of DHA by electron-withdrawing groups. The majority of the substituents' shifts (blue or red) are usually within 10 nm of the parent DHA's spectrum. Maximum red-shifting of 8- and 6-chlorocarbonyl substituted DHAs (+23 and +21 nm, respectively) is observed.

In conclusion, testing various substituents has shown that a spectral nonoverlap can be achieved more effectively when electron-donating groups are introduced at positions other than 8a and 4. This causes a substantial red shift in the VHF UV−vis spectra, particularly methylation of OH and NH_2 groups, which supports our previous finding.

3.3. Hyperpolarizability of Substituted DHA−VHF. In the literature, there are various methods for enhancing the nonlinear optical response of both organic and inorganic systems. The electron push−pull mechanism proves to be an effective method for achieving significant (NLO) responses in organic compounds. In comparison to DHA, VHF has significant charge separation and some zwitterionic properties, which can contribute to a system with a significantly greater NLO response than DHA. Otherwise, DHA has a closed structure without any charge separation, leading to a predicted low NLO response. In VHF, the cyanide group withdraws electrons from the seven-membered ring, resulting in charge separation. Increased hyperpolarizability is a result of a push−pull mechanism, which is very similar to the effect of charge separation. In addition, conjugation is continuous in the VHF form, whereas it is partially interrupted in the DHA form. Furthermore, a low hyperpolarizability value of DHA (5) can be attributed to the fact that it is bent away from planarity. The calculated hyperpolarizabilities, which accurately measure the NLO response, match the predicted values. The parent non-phenyl DHA and VHF have hyperpolarizabilities of 0.55 and 11.3 esu, respectively, according to the calculations.

DHA and VHF have different effects on the NLO response due to substituents. As we reported in our previous study, the hyperpolarizabilities of the system increase whenever a substitution is made on the DHA skeleton. We see here in this research that the hyperpolarizabilities of 8a- PH_2, 8- PH_2, 7- PH_2, 6- PH_2, 5- PH_2, and 4- PH_2 DHAs are 1.40, 1.37, 0.70, 2.17, 2.08, and 1.83 esu, respectively (Table 3). The highest hyperpolarizabilities for all DHA and VHF 6-substituted systems are calculated, quite similar to other electron-donating substituents that were studied before. In the case of VHF, the

hyperpolarizabilities decrease first and then increase, reaching their peak for 5-substituted VHFs. The hyperpolarizabilities of VHFs 8a- PH_2, 8- PH_2, 7- PH_2, 6- PH_2, 5- PH_2, and 4- PH_2 are 11.09, 10.71, 11.37, 11.96, 12.40, and 12.25 esu, respectively (Table 3). The highest value of hyperpolarizabilities is of VHFs at position 5. Because of the reasons stated above, the hyperpolarizabilities of substituted VHFs are higher than those of the corresponding DHAs. The hyperpolarizabilities are calculated to be the lowest for DHA at position 7. When it comes to VHFs, the values that are calculated to be lowest are typically for 8-substituted VHFs.

Methylation of OH and NH_2 generally leads to an increase in hyperpolarizability (for both DHA and VHF), but many exceptions do exist (Table 3). Moreover, for CH_2X DHA and VHFs, the introduction of the additional X group has subtle effects, and it is not trivial to segregate the effects of the additional X moiety.

Quite a remarkable effect is observed when negative charge-bearing moieties (O^- and S^-) are introduced on the DHA skeleton (Table S4). For DHA, the highest hyperpolarizability is calculated for 8a-O^- DHA (29.39 esu). The hyperpolarizabilities of 8-O^-, 7-O^-, 6-O^-, 5-O^-, and 4-O DHAs are 7.44, 12.86, 13.01, 14.43, and 6.07 esu, respectively. The hyperpolarizabilities of S^--substituted DHA systems are lower than the corresponding O^--substituted DHAs. However, a reverse situation is observed for VHFs where the hyperpolarizability of S^--substituted systems is higher than the corresponding O^--substituted VHFs. The highest calculated hyperpolarizability for 6-S^- VHF is 51.65 esu. Similarly, when positive charge-bearing species (NH_3^+ and PH_3^+) are introduced onto the DHA skeleton, the highest hyper-polarizability is calculated for 6-PH_3^+ DHA (13.45 esu). In the case of VHF, PH_3^+ has higher values than the corresponding NH_3^+. However, a reverse situation is observed at position 8; NH_3^+ has a higher value than PH_3^+, which was the highest calculated hyperpolarizability (11.42 esu) (Table S4).

Furthermore, the hyperpolarizabilities of both DHA and VHF in the presence of electron-withdrawing group sub-stituents have been investigated (Table 4). For instance, the hyperpolarizabilities of DHAs with substituents 8a-C(O)Me, 8-C(O)Me, 7-C(O)Me, 6-C(O)Me, 5-C(O)Me, and 4-C(O)Me are 1.48, 2.10, 0.76, 4.99, 2.19, and 2.26 esu, respectively. Meanwhile, the hyperpolarizabilities of VHFs with substituents 8a-C(O)Me, 8-C(O)Me, 7-C(O)Me, 6-C(O)Me, 5-C(O)Me, and 4-C(O)Me are 12.28, 11.48, 11.76, 8.02, 6.88, and 14.15 esu. This clearly shows that for all electron-

withdrawing substituents, 6-substituted DHAs and VHFs have the highest hyperpolarizabilities, while 7-substituted DHAs and VHFs have the lowest hyperpolarizabilities (only with a few exceptions).

To summarize, the hyperpolarizabilities of all substituted VHFs are greater than those of the equivalent DHAs for the reason stated previously. Additionally, the greatest hyperpolarizabilities for DHA and VHF 6-substituted systems are calculated.

4. CONCLUSIONS

In conclusion, the influence of substitution on the absorption properties of DHA−VHF at the seven-membered ring is described, and it is observed that the maximum red shift of DHA−VHF absorption spectra occurs when the conjugation is stabilized by an electron-donating group. Moreover, at positions 4 and 8a, steric hindrance causes a planarity deformation which lowers the conjugation. On the other hand, any electron-drawing group, particularly at the 4 and 8a positions, would result in a blue shift. The loss of planarity and the subsequent decrease in electronic conjugation within the molecule cause a blue shift in the maximum absorption when bulky groups are presented at position 8a. The hyperpolarizabilities of all substituted VHFs are greater than those of their corresponding DHAs, as a result of charge separation; this contributes to a much greater NLO response. Moreover, the highest hyperpolarizabilities for all DHA and VHF 6-substituted systems are calculated.

The theoretical research presented in this study provides a promising avenue for the development of nonlinear optical materials and phototunable absorption. The findings demonstrate the potential for engineering the electronic and optical properties of materials through the manipulation of their molecular structure. Additionally, the development of computational tools to efficiently screen and optimize the design of these materials could accelerate the discovery process and enable the realization of novel functionalities. Overall, the results of this study highlight the potential for nonlinear optical materials and phototunable absorption to contribute to a range of applications in fields such as optoelectronics, telecommunication, and sensing.

■ ASSOCIATED CONTENT

Ⓢ Supporting Information

The Supporting Information is available free of charge at https://pubs.acs.org/doi/10.1021/acsomega.3c01456.

Figure S1: calculated UV−vis spectra for selected 8a-EDG-substituted VHF photoswitches (page S1); Figure S2: calculated UV−vis spectra for different positions of methylation of NHMe VHF photoswitches (page S3); Figure S3: optimized structures of selected methylation of (A) NH_2 and (B) OH VHFs including Φ_1 (page S4); Figure S4: calculated UV−vis spectra of different positions for OMe-VHF photoswitches (page S5); Figure S5: calculated UV−vis spectra of different positions for deprotonated VHFs (S^-) (page S6); Figure S6: geometric properties for deprotonated 4-, 8- and 8a-$O^{(-)}$ (A) and $S^{(-)}$ (B) VHFs indicating the dihedral angle Φ_1 (page S6); Figure S7: calculated UV−vis spectra of different positions for CH2F-VHF photoswitches (page S7); Figure S8: calculated UV−vis spectra of different positions for CH2Br-VHF photo-

switches (page S7); Figure S9: calculated UV−vis spectra of different positions for CH_2Cl-VHF photoswitches (page S7); Figure S10: calculated UV−vis spectra of different positions for CH_2NH_2-VHF photoswitches (page S8); Figure S11: calculated UV−vis spectra of different positions for CH_2OH -VHF photoswitches (page S8); Figure S12: geometric properties for selected (A) CH_2NH_2- and (B) CH_2OH-substituted VHFs (page S8); Figure S13: geometric properties for selected positions of substituted VHFs indicating Φ_1 and Φ_2: (A) NO2, (B) CN, (C) CHO, and (D) COOH (page S9); Figure S14: geometric properties for selected positions of $CONH_2$-substituted VHFs indicating Φ_1 and Φ_2 (page S9); Figure S15: geometric comparison for 8- (a) and 8a-CH_3 (b), 8- (c) and 8a-SiH_3, and (e) 8- (f) and 8a-PH_2 (d) DHA photoswitches indicating Φ_2 (page S10); Figure S16: geometric comparison for 8- (a) and 8a-NH_3^+ (b) and 8- (c) and 8a-PH_3^+ (d) DHA photoswitches indicating Φ_2 (page S10); Table S1: λ_{high} and λ_{max} for DHAs and VHFs (electron-donating groups—*⟨C2−C3−C3a−C8 of DHAs) (page S2); Table S2: percentage contributions of the HOMO (H)−LUMO (L) electronic transition; Table S3: λ_{high} and λ_{max} for DHAs and VHFs (ionic substituents—*⟨C2−C3−C3a−C8 of DHAs) (page S4); and Table S4: hyperpolarizability values for DHAs and VHFs (ionic substituents) (page S10) (PDF)

■ AUTHOR INFORMATION

Corresponding Authors

Imene Bayach − *Department of Chemistry, College of Science, King Faisal University, Al-Ahsa 31982, Saudi Arabia;* ⓘ orcid.org/0000-0003-1375-0612; Phone: +966 13 589 9385; Email: ibayach@kfu.edu.sa

Khurshid Ayub − *Department of Chemistry, COMSATS University, Abbottabad Campus, Abbottabad 22060, Pakistan;* ⓘ orcid.org/0000-0003-0990-1860; Phone: +92 99 238 3591; Email: khurshid@cuiatd.edu.pk; Fax: +92 99 238 3441

Nadeem S. Sheikh − *Chemical Sciences, Faculty of Science, Universiti Brunei Darussalam, Gadong BE1410, Brunei Darussalam;* ⓘ orcid.org/0000-0002-0716-7562; Phone: +673 246 0922/3; Email: nadeem.sheikh@ubd.edu.bn

Authors

Nadiah Almutlaq − *Department of Chemistry, College of Science, King Faisal University, Al-Ahsa 31982, Saudi Arabia*

Mohammed A. Alkhalifah − *Department of Chemistry, College of Science, King Faisal University, Al-Ahsa 31982, Saudi Arabia*

Misbah Asif − *Department of Chemistry, COMSATS University, Abbottabad Campus, Abbottabad 22060, Pakistan*

Complete contact information is available at:
https://pubs.acs.org/10.1021/acsomega.3c01456

Author Contributions

‖I.B. and N.A. contributed equally to this work.

Notes

The authors declare no competing financial interest.

■ ACKNOWLEDGMENTS

■ REFERENCES

(1) Szymański, W.; Beierle, J. M.; Kistemaker, H. A. V.; Velema, W. A.; Feringa, B. L. Reversible Photocontrol of Biological System by the Incoporaton of Molecular Photoswitches. *Chem. Rev.* **2013**, *113*, 6114−6178.

(2) Saima, B.; Khan, N.; Al-Faiyz, Y. S. S.; Ludwig, R.; Rehman, W.; Habib-ur-Rehman, M.; Sheikh, N. S.; Ayub, K. Photo-tunable linear and nonlinear optical response of cyclophanediene-dihydropyrene photoswitches. *J. Mol. Graphics Modell.* **2019**, *88*, 261−272.

(3) Plaquet, A.; Champagne, B.; Castet, F.; Ducasse, L.; Bogdan, E.; Rodriguez, V.; Pozzo, J.-L. Theoretical Investigation of the Dynamic First Hyperpolarizability of DHA-VHF Molecular Switches. *New J. Chem* **2009**, *33*, 1349−1356.

(4) Kariduraganavar, M. Y.; Doddamani, R. V.; Waddar, B.; Parne, S. R. Nonlinear Optical Responsive Molecular Switches. *IntechOpen* **2021**, DOI: 10.5772/intechopen.92675.

(5) Irie, M. Diarylethene for Memories an Switches. *Chem. Rev.* **2000**, *100*, 1685−1716.

(6) Chan, J. C.-H.; Lam, W. H.; Yam, V. W.-W. A Highly Efficient Silole-Containing Dithienylethene with Excelent Thermal Stability and Fatigue Resistance: A Promisng Candidate for Optical Memory Storage Materials. *J. Am. Chem. Soc.* **2014**, *136*, 16994−16997.

(7) Fortin, D. L.; Banghart, M. R.; Dunn, T. W.; Borges, K.; Wagenaar, D. A.; Gaudry, Q.; Karakossian, M. H.; Otis, T. S.; Kristan, W. B.; Trauner, D.; Kramer, R. H. Photochemical Control of Endogenous Ion Channels and Cellular Excitability. *Nat. Methods* **2008**, *5*, 331−338.

(8) Hoppmann, C.; Seedorff, S.; Richter, A.; Fabian, H.; Schmieder, P.; R″uck-Braun, K.; Beyermann, M. Light-Directed Protein Binding of a Biological Relevant β-Sheet. *Angew. Chem., Int. Ed.* **2009**, *48*, 6636−6639.

(9) Kawata, S.; Kawata, Y. Three-Dimensional Optical Data Storage Using Photochromic Materials. *Chem. Rev.* **2000**, *100*, 1777−1788.

(10) Liang, X.; Mochizuki, T.; Asanuma, H. A Supra-Photoswitch Involving Sandwiched DNA Base Pairs and Azobenzenes for Light-Driven Nanostructures and Nanodevices. *Small* **2009**, *5*, 1761−1768.

(11) Matharu, A. S.; Jeeva, S.; Ramanujam, P. S. Liquid Crystals for Holographic Optical Data Storage. *Chem. Soc. Rev.* **2007**, *36*, 1868−1880.

(12) Raymo, F. M.; Tomasulo, M. E. Electron and Energy Transfer Modulation with Photochromic Switches. *Chem. Soc. Rev.* **2005**, *34*, 327−336.

(13) Sadovski, O.; Beharry, A. A.; Zhang, F.; Woolley, G. A. Spectral Tuning of Azobenzene Photoswitches for Biological Applications. *Angew. Chem., Int. Ed.* **2009**, *48*, 1484−1486.

(14) Tian, H.; Yang, S. Recent Progresses on Diarylethene Based Photochromic Switches. *Chem. Soc. Rev.* **2004**, *33*, 85−97.

(15) Volgraf, M.; Gorostiza, P.; Numano, R.; Kramer, R. H.; Isacoff, E. Y.; Trauner, D. Allosteric Control of an Ionotropic Glutamate Receptor with an Optical Switch. *Nat. chem. Biol.* **2006**, *2*, 47−52.

(16) Whalley, A. C.; Steigerwald, M. L.; Guo, X.; Nuckolls, C. Reversible Switching in Molecular Electronic Devices. *J. Am. Chem. Soc.* **2007**, *129*, 12590−12591.

(17) Yagai, S.; Kitamura, A. Recent Advances in Photoresponsive Supramolecular Self-Assemblies. *Chem. Soc. Rev.* **2008**, *37*, 1520−1529.

(18) Bousquet, D.; Peltier, C.; Masselin, C.; Jacquemin, D.; Adamo, C.; Ciofini, I. A DFT Study of Magnetic Interactions in Photoswitchable Systems. *Chem. Phys. Lett.* **2012**, *542*, 13−18.

(19) Datta, S. N.; Pal, A. K.; Hansda, S.; Latif, I. A. On the Photomagnetism of Nitronyl Nitroxide, Imino Nitroxide, and Verdazyl-Substituted Azobenzene. *J. Phys. Chem. A* **2012**, *116*, 3304−3311.

(20) Matsuda, K.; Matsuo, M.; Mizoguti, S.; Higashiguchi, K.; Irie, M. Reversed Photoswitching of Intramolecular Magnetic Interaction Using A Photochromic Bis(2-Thienyl)ethene Spin Coupler. *J. Phys. Chem. B* **2002**, *106*, 11218−11225.

(21) Kobuke, Y.; Ohgoshi, A. Supramolecular Ion Channel Containing Trans-Azobenzene for Photocontrol of Ionic Fluxes. *Colloids. Surf. Physicochem. Eng. Asp.* **2000**, *169*, 187−197.

(22) Woolley, G. A. N. Neurochemistry: Lighting up with Azobenzenes. *Nat. Chem.* **2012**, *4*, 75−77.

(23) Lubbe, A. S.; Szymanski, W.; Feringa, B. L. Recent Developments in Reversible Photoregulation of Oligonucleotide Structure and Function. *Chem. Soc. Rev.* **2017**, *46*, 1052−1079.

(24) Lerch, M. M.; Hansen, M. J.; van Dam, G. M.; Szymanski, W.; Feringa, B. L. Emerging Targets in Photopharmacology. *Angew. Chem., Int. Ed.* **2016**, *55*, 10978−10999.

(25) Andréasson, J.; Kodis, G.; Terazono, Y.; Liddell, P. A.; Bandyopadhyay, S.; Mitchell, R. H.; Moore, T. A.; Moore, A. L.; Gust, D. Molecule-Based Photonically Switched Half-Adder. *J. Am. Chem. Soc.* **2004**, *126*, 15926−15927.

(26) Andréasson, J.; Straight, S. D.; Kodis, G.; Park, C. Do.; Hambourger, M.; Gervaldo, M.; Albinsson, B.; Moore, T. A.; Moore, A. L.; Gust, D. All-Photonic Molecular Half-Adder. *J. Am. Chem. Soc.* **2006**, *128*, 16259−16265.

(27) Prasanna De Silva, A.; McClenaghan, N. D. Proof-of-Principle of Molecular-Scale Arithmetic. *J. Am. Chem. Soc.* **2000**, *122*, 3965−3966.

(28) Guo, X.; Zhang, D.; Zhang, G.; Zhu, D. Monomolecular Logic: "Half-Adder" Based on Multistate/Multifunctional Photochromic Spiropyrans. *J. Phys. Chem. B* **2004**, *108*, 11942−11945.

(29) Margulies, D.; Melman, G.; Felder, C. E.; Arad-Yellin, R.; Shanzer, A. Chemical Input Multiplicity Facilitates Arithmetical Processing. *J. Am. Chem. Soc.* **2004**, *126*, 15400−15401.

(30) Qu, D.-H.; Wang, Q.-C.; Tian, H. A Half Adder Based on a Photochemically Driven [2]Rotaxane. *Angew. Chem., Int. Ed.* **2005**, *44*, 5296−5299.

(31) Remacle, F.; Weinkauf, R.; Levine, R. D. Molecule-Based Photonically Switched Half and Full Adder. *J. Phys. Chem. A* **2006**, *110*, 177−184.

(32) Stojanović, M. N.; Stefanović, D. Deoxyribozyme-Based Half-Adder. *J. Am. Chem. Soc.* **2003**, *125*, 6673−6676.

(33) Zhou, Y.; Wu, H.; Qu, L.; Zhang, D.; Zhu, D. A New Redox-Resettable Molecule-Based Half-Adder with Tetrathiafulvalene. *J. Phys. Chem. B* **2006**, *110*, 15676−15679.

(34) Budyka, M. F. Molecular switches and logic gates for information processing, the bottom-up strategy: from silicon to carbon, from molecules to supermolecules. *Russ. Chem. Rev.* **2017**, *86*, 181.

(35) Andréasson, J.; Straight, S. D.; Moore, T. A.; Moore, A. L.; Gust, D. Molecular All-Photonic Encoder−Decoder. *J. Am. Chem. Soc.* **2008**, *130*, 11122−11128.

(36) Gierisch, S.; Daub, J. Lichtsensitive Dihydroazulene: Alternativer Syntheseweg − Einfluß von Alkylsubstituenten im Fünfring auf das photochrome Verhalten. *Chem. Ber.* **1989**, *122*, 69−75. *Chem. Ber.* **1989**, *122*, 69

(37) Åxman Petersen, M.; Zhu, L.; Jensen, S. H.; Andersson, A. S.; Kadziola, A.; Kilså, K.; Brøndsted Nielsen, M. Photoswitches Containing a Dithiafulvene Electron Donor. *Adv. Funct. Mater.* **2007**, *17*, 797−804.

(38) Daub, J.; Gierisch, S.; Klement, U.; Knöchel, T.; Maas, G.; Seitz, U. Lichtinduzierte reversible Reaktionen: Synthesen und Eigenschaften photochromer 1,1-Dicyan-1,8a-dihydroazulene und thermochromer 8-(2,2-Dicyanvinyl)heptafulvene. *Chem. Ber.* **1986**, *119*, 2631−2646.

(39) Daub, J.; Knöchel, T.; Mannschreck, A. Photosensitive Dihydroazulenes with Chromogenic Properties. *Angew. Chem., Int. Ed.* **1984**, *23*, 960−961.

(40) Gierisch, S.; Bauer, W.; Burgemeister, T.; Daub, J. Der Einfluß von Substituenten auf die Photochromie Dihydroazulen ⇆ Dicyanvinylheptafulven: Sterische und elektronische Effekte bei 9-Anthrylverbindungen — Synthese von kondensierten Hydropentalenen. *Chem. Ber.* **1989**, *122*, 2341−2349.

(41) Gobbi, L.; Seiler, P.; Diederich, F. A Novel Three-Way Chromophoric Molecular Switch: pH and Light Controllable Switching Cycles. *Angew. Chem., Int. Ed.* **1999**, *38*, 674−678.

(42) Petersen, M. Å.; Andersson, A. S.; Kilså, K.; Nielsen, M. B. Redox-Controlled Dihydroazulene-Vinylheptafulvene Photoswitch Incorporating Tetrathiafulvalene. *Eur. J. Org. Chem.* **2009**, *2009*, 1855−1858.

(43) Spreitzer, H.; Daub, J. Functional Dyes for Molecular Switching. Dihydroazulene/vinylheptafulvene Photochromism: Effect of π-Arylenes on the Switching Behavior. *Liebigs Ann.* **1995**, *1995*, 1637−1641.

(44) Spreitzer, H.; Daub, J. Multi-Mode Switching Based on Dihydroazulene/vinylheptafulvene Photochromism: Synergism of Photochromism and Redox Switching in Heteroaryl-Functionalized Systems. *Chem. — Eur. J.* **1996**, *2*, 1150−1158.

(45) Bouas-Laurent, H.; Dürr, H. Organic Photochromism (IUPAC Technical Report). *Pure Appl. Chem.* **2001**, *73*, 639−665.

(46) Mrozek, T.; G″orner, H.; Daub, J. Multimode-Photochromism Based on Strongly Coupled Dihydroazulene and Diarylethene. *Chem. — Eur. J.* **2001**, *7*, 1028−1040.

(47) Broman, S. L.; Petersen, MÅ.; Tortzen, C. G.; Kadziola, A.; Kilså, K.; Nielsen, M. B. Arylethynyl Derivatives of the Dihydroazulene/Vinylheptafulvene Photo/Thermoswitch: Tuning the Switching Event. *J. Am. Chem. Soc.* **2010**, *132*, 9165−9174.

(48) Petersen, M. Å.; Broman, S. L.; Kadziola, A.; Kilså, K.; Nielsen, M. B. Dihydroazulene Photoswitches: The First Synthetic Protocol for Functionalizing the Seven-Membered Ring. *Eur. J. Org. Chem.* **2009**, *2009*, 2733−2736.

(49) Petersen, M. Å.; Broman, S. L.; Kilså, K.; Kadziola, A.; Kadziola, A.; Nielsen, M. B. Gaining Control: Direct Suzuki Arylation of Dihydroazulenes and Tuning of Photo- and Thermochromism. *Eur. J. Org. Chem.* **2011**, *2011*, 1033−1039.

(50) Shahzad, N.; Nisa, R. U.; Ayub, K. Substituents Effect on Thermal Electrocyclic Reaction of Dihydroazulene−vinylheptafulvene Photoswitch: A DFT Study to Improve the Photoswitch. *Struct. Chem.* **2013**, *24*, 2115−2126.

(51) Bayach, I.; Al-faiyz, Y. S. S.; Alkhalifah, M. A.; Almutlaq, N.; Ayub, K.; Sheikh, N. S. Phototunable Absorption and Nonlinear Optical Properties of Thermally Stable Dihydroazulene−Vinyl-heptafulvene Photochrome Pair. *ACS Omega* **2022**, *7*, 35863−35874.

(52) Hansen, M. H.; Elm, J.; Olsen, S. T.; Gejl, A. N.; Storm, F. E.; Frandsen, B. N.; Skov, A. B.; Nielsen, M. B.; Kjaergaard, H. G.; Mikkelsen, K. V. Theoretical Investigation of Substituent Effects on the Dihydroazulene/Vinylheptafulvene Photoswitch: Increasing the Energy Storage Capacity. *J. Phys. Chem. A* **2016**, *120*, 9782−9793.

(53) Frisch, M. J.; Trucks, G. W.; Schlegel, H. B.; Scuseria, G. E.; Robb, M. A.; Cheeseman, J. R.; Scalmani, G.; Barone, V.; Mennucci, B.; Petersson, G. A. et al.*Gaussian 09*; Gaussian, Inc.: Wallingford CT, 2009.

(54) Bano, R.; Arshad, M.; Mahmood, T.; Ayub, K.; Sharif, A.; Perveen, S.; Tabassum, S.; Yang, J.; Gilani, M. A. Face specific doping of Janus all-cis-1, 2, 3, 4, 5, 6-hexafluorocyclohexane with superalkalis and alkaline earth metals leads to enhanced static and dynamic NLO responses. *J. Phys. Chem. Solids* **2022**, *160*, No. 110361.

(55) Mitchell, R. H.; Bohne, C.; Robinson, S. G.; Yang, Y. The Effect of Addition of Fluorescent Moieties to Dihydropyrenes: Enhancing Photochromicity and Fluorescence Monitoring. *J. Org. Chem.* **2007**, *72*, 7939−7946.

(56) Perrier, A.; Maurel, F.; Jacquemin, D. Diarylethene−dihydroazulene Multimode Photochrome: A Theoretical Spectroscopic Investigation. *Phys. Chem. Chem. Phys.* **2011**, *13*, 13791−13799.